Atmos. Meas. Tech. Discuss., doi:10.5194/amt-2016-320, 2016
Manuscript under review for journal Atmos. Meas. Tech.
Published: 7 October 2016

Atmospheric Measurement Techniques
Discussions

VHF antenna pattern characterization by the observation of meteor head echoes.

Toralf Renkwitz[1], Carsten Schult[1], and Ralph Latteck[1]

[1]Leibniz-Institute of Atmospheric Physics, Schloss-Str. 6, 18225 Kuehlungsborn

Correspondence to: Toralf Renkwitz (renkwitz@iap-kborn.de)

Abstract. The Middle Atmosphere Alomar Radar SYstem (MAARSY) with its active phased array antenna is designed and used for studies of phenomena in the mesosphere and lower atmosphere. The flexible beam forming and steering combined with a large aperture array allows observations with high temporal and angular resolution. For both, the analysis of the radar data and the configuration of experiments, the actual radiation pattern needs to be known. For that purpose various simulations as well as passive and active experiments have been conducted. Here, results of meteor head echo observations are presented, which allow derivation of detailed information of the actual radiation pattern for different beam pointing positions and the current health status of the entire radar. For MAARSY, the described method offers robust beam pointing and width estimations for a minimum of a few days of observations.

1 Introduction

The Middle Atmosphere Alomar Radar System (MAARSY) was built in 2009/2010 by the Leibniz-Institute of Atmospheric Physics (IAP) on the North Norwegian island Andøya (69.3°N, 16.04°E) to allow improved studies of various atmospheric heights at high spatial and temporal resolution. Main target regions are the troposphere/lower stratosphere and the mesosphere. MAARSY's main active phased antenna array consists of 433 yagi antennas (see Figure 1), which are connected to their individual transceiver module allowing independent phase and amplitude control. Such a configuration allows both flexible pulse-to-pulse steering and forming of the radar beam by appropriate selection of amplitude and phase distribution over the array elements. A detailed description of the radar and its properties are given by *Latteck et al.* (2012), while recent geophysical investigations with MAARSY regarding layered phenomena in the mesosphere have been presented in *Latteck and Strelnikova* (2015) and *Sommer et al.* (2016).

The knowledge of the current radiation pattern characteristics is important for both the design of experiments, e.g. specific experiment settings, and even more crucial for the analysis of radar data. The most important points to know are the beam pointing accuracy, shape and width of the beam, the antenna gain and the position and intensity of side lobes.

For the validation of MAARSY's radiation pattern various passive and active experiments were already conducted. In passive experiments cosmic radio emissions from our galaxy as well as distinct radio sources like radio galaxies, supernova remnants and the diffuse background were observed. Subsequently, the derived intensity maps covering from 10 to 90° of northern declination were compared to the detailed Global Sky Temperature model by *de Oliveira-Costa et al.* (2008) as a reference

Atmos. Meas. Tech. Discuss., doi:10.5194/amt-2016-320, 2016
Manuscript under review for journal Atmos. Meas. Tech.
Published: 7 October 2016

map by involving the simulated radiation pattern of MAARSY. The simulation of MAARSY's radiation pattern considering the mechanical structure, soil properties and antenna coupling were performed using the well accepted Numerical Electromagnetic Code (NEC 4.1) for different arctic weather situations. Doing so, we were able to derive the pointing accuracy and beam width for different antenna array sizes (*Renkwitz et al.*, 2012) and estimated the antenna array gain by knowing the absolute intensity flux of the observed radio sources (*Renkwitz*, 2014). Furthermore, the observation of distinct radio sources like Cassiopeia A allow absolute phase calibration for the individual subgroups of an antenna array as described for MAARSY in *Chau et al.* (2014). The knowledge of the individual antenna array subgroups phases is essential for the integration to synthetic arrays providing different beam shapes and widths as well as the interferometric analysis of the data to e.g. locate the mean angle of arrival of the radar echo.

Additionally, active experiments were conducted in which the Earth's moon and large artificial satellites were used as radar targets as described in *Renkwitz et al.* (2013) as well as more recently scattering off a sounding rocket's payload (*Renkwitz et al.*, 2015). In general, these experiments have shown a good agreement to the simulated radiation pattern, though there have been found some discrepancies in the estimated beam widths and negligible inaccuracy of the beam pointing. The cause for the slightly increased beam width was assumed to be a matter of the existent mixed polarization during the system upgrade in 2012/2013 converting from linear to circular polarization. This widening of the radiation pattern was also indicated in thorough NEC simulations.

In this paper we present the methodology that have been used to augment our knowledge of the actual three-dimensional radiation pattern of the MAARSY radar by analyzing meteor head echo observations. Here, the main aim is to present a robust approach to estimate and validate the simulated radiation pattern using the angularly resolved statistical distribution of meteor head echo trajectories.

For specular meteor radars, the angular distribution of detected trails allows to map the general coverage of the used radars. This coverage distribution can be seen in wide beam meteor radars using e.g. one single beam, multiple beams like the SAAMER/DRAAMER installations (*Fritts et al.*, 2010, 2012), but also for narrow beam antenna arrays like the MU radar *Nakamura et al.* (1991). The observation of specular meteors, however, does not allow the derivation of the actual beam shape, but gives an indication of the maximum radial coverage off the nominal pointing direction. This is caused by the necessity of having perpendicularity between the emitted radio wave and the meteor trajectory. Due to this requirement only a subset of all existing meteors are seen by a single monostatic specular meteor radar. Furthermore, most of the specular meteor trajectories are typically seen around 50° elevation angle and below due to the increasing observation volume for the meteor ablation heights. Especially, for the zenith-near directions the geometry for suitable meteor trajectories perpendicular to the radio wave are very limited. Thus, the angular statistical appearance of specular meteors trajectories cannot be used for the beam pattern validation.

But, the perpendicularity requirement does not hold for the observation of meteor head echoes, which therefore could be used to map the radiation pattern by the angular distribution of detected echoes for a certain amount of time. Meteor head echoes, however, are severely weaker than specular meteor echoes scattering off the meteor trail and therefore high-power large-aperture radars are needed to compensate for the lower efficiency of this scattering process. Meteor head observations are described

Atmos. Meas. Tech. Discuss., doi:10.5194/amt-2016-320, 2016
Manuscript under review for journal Atmos. Meas. Tech.
Published: 7 October 2016

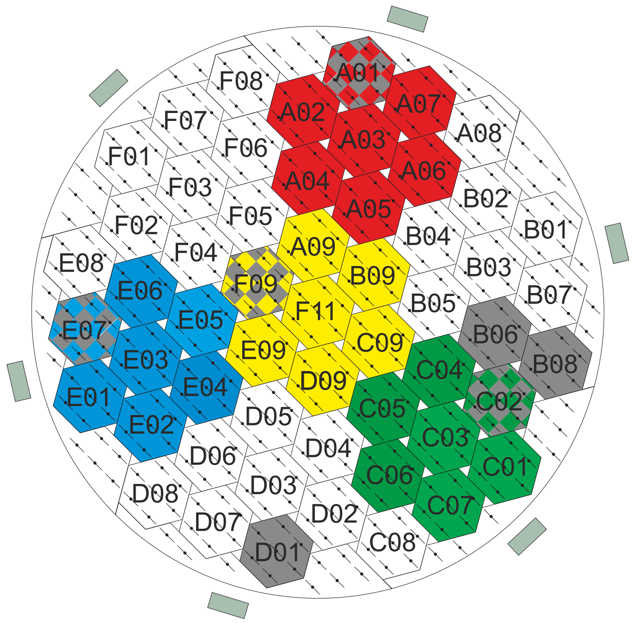

Figure 1. Sketch of MAARSY's main antenna array, consisting of 433 yagi antennas. The Anemone subarray groups A, C, E and M, each composed of 49 antennas, are individually color-coded, while 7 antennas form a Hexagon, e.g. D-01. Besides the total antenna array, the subarray groups marked in color are used for reception in the examined experiment mst006.

for various radar system of sufficient power-aperture product in e.g. *Pellinen-Wannberg and Wannberg* (1994); *Janches et al.* (2000); *Chau and Woodman* (2004); *Pellinen-Wannberg* (2005); *Chau et al.* (2009); *Kero et al.* (2011); *Schult et al.* (2013). In the following section meteor head echo observations with MAARSY are briefly described, followed by the methodology of this experiment using meteor head echo observations for radiation pattern validation. The proposed method is shown for two case studies in which MAARSY was operational with the entire antenna array and for a short period when about 20% of the array were non-functional resulting in a distorted radiation pattern. The results underline the exceptional value of this analysis to monitor the health status of the radar as a byproduct of routine observations. Finally, a discussion and conclusions are given.

1.1 Meteor head echo observations with MAARSY

The MAARSY radar is one of the few radar systems that are capable of routinely observing meteor head echoes as described in *Schult et al.* (2013), offering a power-aperture product of 9.7MWm^2. Meteor head echo observations are performed with either specialized or multi-purpose experiments. The most interesting details of the multi-purpose experiment used during the examined period are shown in Table 1. Within this experiment both the troposphere and mesosphere region were monitored altogether. The echo intensity is typically derived for the entire antenna array, while the radial and angular position of the meteor head echo trajectories are derived by interferometric means using smaller subarrays. For transmission the entire antenna

parameter	value
pulse repetition frequency	1000 Hz
range resolution	450 m
sampling range	$\approx$ 7 - 148 km
beam directions	$\phi = 0°$, $\theta = 0°$; $\phi = 185°$, $\theta = 12.4°$
pulse code	16-bit complementary
coherent integration	2
Nyquist frequency	15.6 Hz
subarray groups	A, Y1, C, Y2, E, Y3, M, A-01, B-06, C-02, D-01 E-07, ALW64, B-08

Table 1. Details of the monitoring experiment mst006 also used to observe meteor head echoes, accompanied by the list of used subarray groups (see Figure 1 for comparison). The antennas Y1, Y2, Y3 and ALW64 are external antennas and are not used in this study.

array was operated at maximum output power (no amplitude taper), for reception various subarrays, Hexagons and Anemones comprised of 7 and 49 antennas respectively, have been used for the interferometric analysis. The benefit of using different sizes of subarrays and the baseline between them is connected to their individual gain and beam width as well as the resulting interferometric unambiguous angular range. The use of closely spaced smaller subarrays (B-06, B-08, C-02, see array sketch in Figure 1), with each 30° beam width, facilitate an unambiguous angular range of approximately 15.6° degrees. In addition, widely spaced Anemone subarrays (A, C, E, M), with each 11° beam width, provide more gain in the main beam direction. Thus, the closely spaced Hexagons permit the rough angular location of the event, while using the Anemones allow the detection of weaker events as well as precise phase and thus position information of the observed target with their longer baseline lengths.

Due to the high velocity of the observed targets the received signals need to be decoded Doppler-corrected for the individual complementary codes to ensure proper reconstruction of the signals and thus the individual meteor trajectory (see e.g. *Kero et al.*, 2012; *Schult et al.*, 2016, and references within).

The detected power of meteor head echoes for the same radar parameters vary significantly from one event to the other due to the meteor's orientation and entry velocity to the Earth atmosphere, its size and composition, which therefore requires normalization of the individual data. First attempts to use normalized meteor head echo intensities for some events observed with MAARSY were compared to simulated radiation pattern cross-sections as described in *Chau et al.* (2014). Here, quite good agreement for the main beam and the first side lobe were found, both in shape and width. However, as previously quoted this approach was limited to the piecewise comparison of few individual meteor trajectories.

Atmos. Meas. Tech. Discuss., doi:10.5194/amt-2016-320, 2016
Manuscript under review for journal Atmos. Meas. Tech.
Published: 7 October 2016

2 Methodology and experiment description

The initial premise for this study was to automatically analyze the trajectory data without additional discrimination or selection of individual meteor head echo events and their trajectories. The detected intensities or better the sufficient signal-to-noise ratio is a necessary requirement for the calculation of the trajectory, but is not used in the subsequent analysis described here. Contrary to the previously mentioned method to infer the two-dimensional radiation pattern from the detected intensities of selected meteor trajectories, here, the statistical occurrence of trajectory points per defined angular bin are used to deduce the three-dimensional radiation pattern.

The assumption is, that as long as the radar parameters, especially beam pointing and width, are not changed significantly, the radiation pattern should be reflected in the angular occurrence of the events. As previously noted, the detectability of meteor head echoes depend on the volume illuminated by the radar and for reception on the selection of subarray groups (beam width, gain), but also on the available baselines to recover the unambiguous position of the meteors. Thus, the angular occurrence, or count rate, of the meteor head echo positions within the given unambiguous angular range is only determined by the actual radiation pattern.

The data we use in this study was collected with the MAARSY radar between December 1st 2013 and February 26th 2014 with the monitoring experiment mst006 (see Table 1). With this experiment radar measurements in two distinct beam directions were performed, pointing towards zenith and off-vertical towards $\phi = 185°$, $\theta = 12.4°$.

For the reliable reconstruction of a meteor's trajectory a minimum of 11 points are defined, but may consists of few hundred points for larger, but rare examples. During the entire period, the average length of derived trajectories accounts for 28 points. For this experiment, the occurrence of all derived meteor trajectory points are calculated for angular bins of a resolution of $0.2\text{x}0.2°$ resolution and ablation heights of 85 to 115km are used. The increasing volume for greater zenith angle off-sets is negligible for zenith near directions, $< 0.1\text{dB}$ for 5°, but more crucial for $\theta = 15°$ accounting for -0.3dB. The resulting occurrence map is smoothed (9-point-median) and interpolated where necessary to derive the complete three-dimensional intensity and shape of the main beam and the first side lobes as well as the beam width.

During the period studied here, on late December 31st one of the six containers housing the radar hardware for the Anemone group F and two Hexagon groups of the center Anemone M got inoperable for both reception and transmission, but operation was restored on late January 7th. This period of restricted operability is individually investigated to underline the reliability and sensitivity of this method.

2.1 Angular occurrence of meteor head echo trajectories for a period of three months

For the nearly three months long period of full functionality, in total, 141118 meteor head echo trajectories, accounting for more than $4 \cdot 10^6$ trajectory points for the zenith beam and the southwards tilted beam were derived and used to generate angular occurrence maps.

The calculated occurrence of meteor trajectories for the zenith pointing radar beam is depicted in Figure 2. The occurrence map is accompanied by contour lines of the simulated combined radiation pattern, 433 and 49 antennas for transmission and

Atmos. Meas. Tech. Discuss., doi:10.5194/amt-2016-320, 2016
Manuscript under review for journal Atmos. Meas. Tech.
Published: 7 October 2016

Atmospheric Measurement Techniques
Discussions

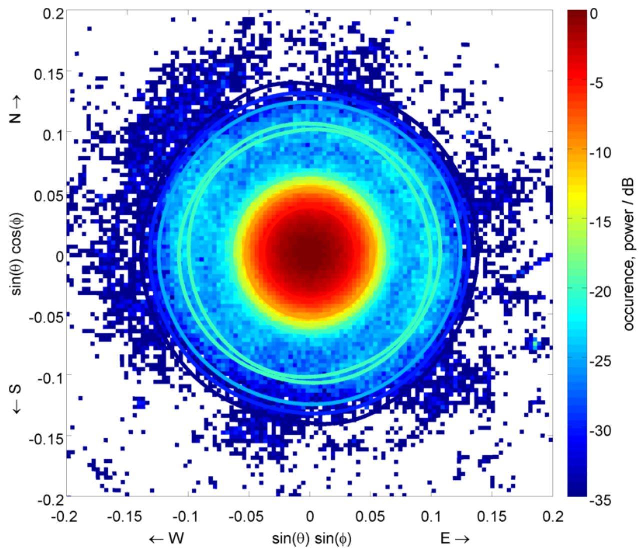

Figure 2. Angular occurrence rate of meteor head echo trajectory points for zenith beam pointing observed with MAARSY during a period of almost three months and overlaid by the simulated radiation pattern.

reception, respectively. While the entire antenna array, superposed of 433 nominal antennas, are used for transmission, the latter 49 antenna subgroups are the largest directly sampled subarrays of MAARSY and are used for the final interferometric examination of the trajectory estimation. Therefore, the total two-way radiation pattern consists of the superposition of both 433 and 49 antennas.

The very similar distribution was derived for the tilted radar beam, pointing to $\phi = 185°$, $\theta = 12.4°$, but is not shown separately as no additional information are apparent. For both cases, the occurrences agree well to the simulated radiation pattern for the main lobe and first side lobe, which is highlighted in Figure 3. There, the cross-sections in the south-north and west-east planes for both beam directions are shown as well as the simulated pattern reference.

The observed beam shape and width for both pointing directions matches the simulations, while a slight broadening is seen for the tilted beam, which is caused be the decrease of effective antenna area. The broadening factor can be estimated by the cosine of the off-boresight pointing, which agrees to the observed broadening of $0.1°$. Besides this, a slight beam pointing error of approximately $0.1°$ towards southwest is visible in the figure.

Precise beam pointing estimation was estimated by the median of the original trajectory points, before sorting the data into $0.2°$ bins. Doing so, the beam pointing positions for the entire period of proper operation, were calculated to $\phi = 246.7°$, $\theta = 0.12°$ and $\phi = 185.6°$, $\theta = 12.47°$ for the zenith pointing and tilted beam, respectively. The offset to the nominal beam pointing may consistently be accounted for both beam directions to $0.12°$ southwest of the initial direction.

Atmos. Meas. Tech. Discuss., doi:10.5194/amt-2016-320, 2016
Manuscript under review for journal Atmos. Meas. Tech.
Published: 7 October 2016

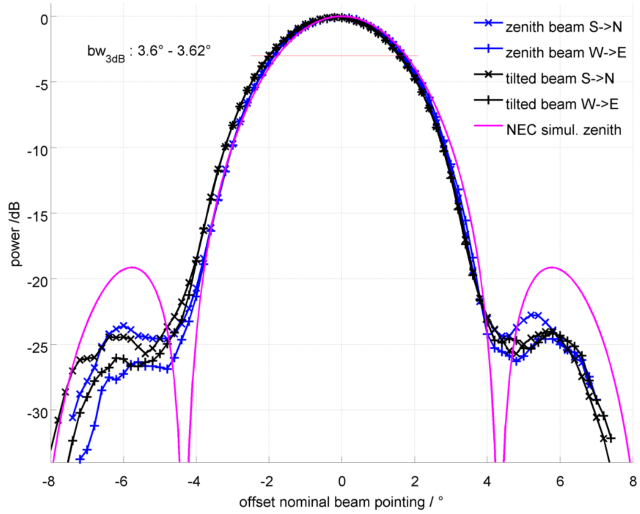

Figure 3. Cross-sections through the angular occurrence rate for both beam pointing directions, $\phi = 0°$, $\theta = 0°$ (blue) and $\phi = 185°$, $\theta = 12.4°$ (black) in respect of their nominal position, compared to the simulated radiation pattern (magenta).

2.2 Estimated radiation pattern for a period of a few days

Contrary to the previous section, where the MAARSY radar was in normal operation using the entire antenna array, here the period from January 1st to late 7th 2014 is investigated. During that period container F failed and therefore 20% of the antenna array were not available (subarray groups F-01 to F-11, see Figure 1). This inoperability is valid for transmission and reception, so for the illumination of the target volume and loss of the Hexagon F-09 that is also sampled for potential interferometric use. The latter does not affect the recovery of the meteor trajectories as that explicit Hexagon is not part of the essential smallest baseline group (B-06, B-08, C-02).

For this period of one week, approximately 250000 reliable trajectory points for each beam pointing direction were derived and analyzed. The occurrence map for this period for the tilted beam is shown in Figure 4, while the vertical beam is equivalent. Equivalently to the earlier figures, the occurrence maps have been superimposed by the simulated radiation pattern. For a horizontal cut through the main beam, equivalently e.g. -13dB contour line (yellow), the normally circular shape of the main beam is clearly deformed to an oval shape due to the large portion of inactive antennas. The longer axis of the oval is oriented along the direction of the missing array elements, northwest - southeast axis, which agrees to the inverse relationship of beam width and maximum extent of incorporated array elements. For both beam directions the occurrence maps appear to be similar in terms of shape and spread around the nominal beam pointing direction. This underlines the proper function of the remaining radar hardware and antenna array in use and allows the detailed analysis shown in Figure 5. In the left panel the cross-section south-north is shown for both beam pointing directions in respect to their nominal beam pointing position, while in the right panel the southwest towards northeast cross-section is depicted. The latter is especially interesting as the prominent side lobes are generated in these directions, seen in both, the observations and the simulations. For both beam pointing directions the

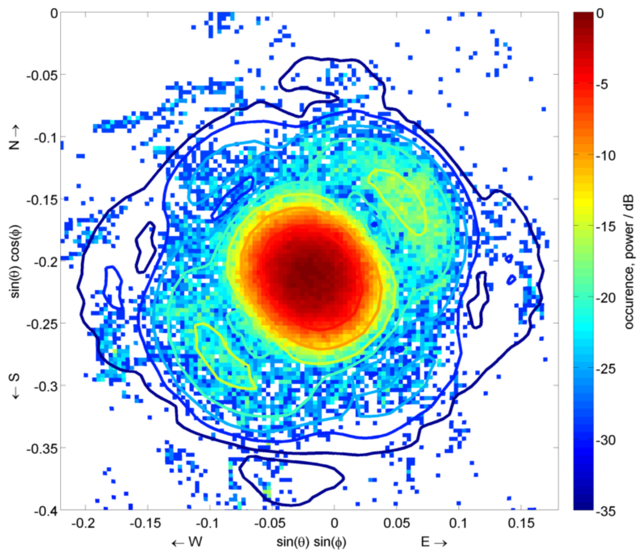

Figure 4. Angular occurrence rate for the tilted beam ($\phi = 185°$, $\theta = 12.4°$) overlaid by the simulated radiation pattern for January 2014, when about 20% of the antenna array was nonfunctional.

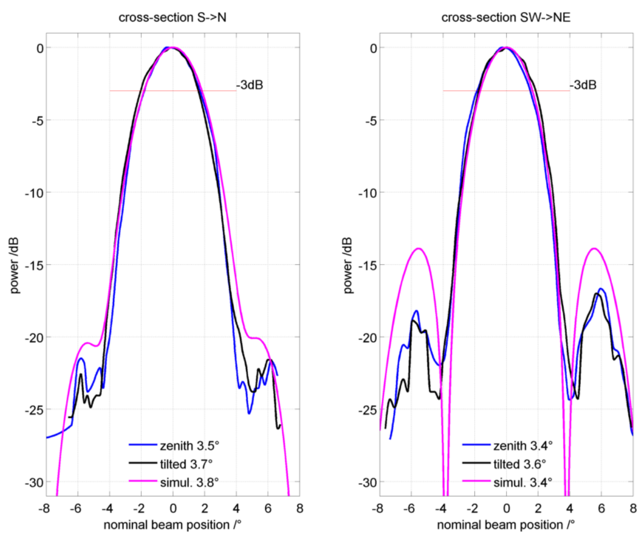

Figure 5. Cross-sections through the angular occurrence rate for both beam directions compared to the simulated radiation pattern for the period of January 1st to 8th 2014. The simulated and estimated beam widths are shown at the bottom.

simulated pattern proposes less side lobe suppression than we actually see in this analysis. Earlier observations scattering off a sounding rocket's payload , however, indicated a better agreement of side lobes' intensity to the simulations. The position of the first null, especially for the SW-NE cross-section, seems to be slightly shifted outward. To complement the earlier findings and underlining the sensitivity of the described method the occurrences of meteor trajectory points for December 15th 2013

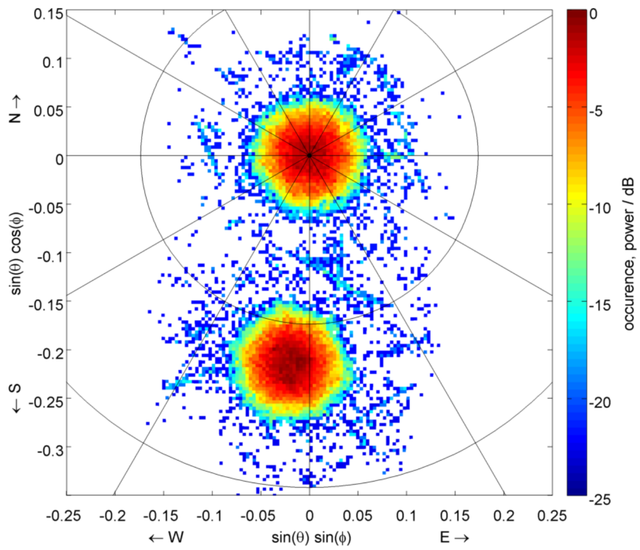

Figure 6. Angular occurrence of meteor head echo trajectory points for the period December 15th 2013 for two beam poiniting directions, $\phi = 0°$, $\theta = 0°$ and $\phi = 185°$, $\theta = 12.4°$.

for both beam pointing directions, $\phi = 0°$, $\theta = 0°$ and $\phi = 185°$, $\theta = 12.4°$ are depicted in Figure 6. On that day about 2850 meteor head echo trajectories, consisting of 82000 points, were derived in total for both beam directions. The high number of detected trajectories and depicted spurs next to the main beam positions are related to the day of these measurements around the maximum of the Geminids meteor shower. The detected distribution already fairly matches the Gaussian like shape of the radiation pattern, though for the precise derivation of parameters like beam width a larger dataset should be used. With the assumption of pattern symmetry and referencing to the center of the beam it would be possible to average the occurrences in azimuth to overcome the low count rates. However, the median beam pointing direction for this single day is estimated to be about $0.17°$ southwestward off the nominal direction, which is in good agreement to the value estimated for the entire period of nearly three months.

3 Discussion

The described method seems to be well suitable to the derive the actual radiation pattern by analyzing the occurrence of meteor head echo trajectory points. For the rough estimation of the pattern we've shown occurrences for just a single day, though it was right in the maximum of the Geminids shower, it proved the principle reliability of the method. Of course, it is certainly recommended to use as much data as available to improve the statistics for both the reconstruction of all individual trajectories and the parameters derived from the total occurrences.

Altogether, the estimated beam widths for the individual periods correspond well to the simulation, though a minor broadening can be distinguished. Broadening can be caused by amplitude tapering, typically used to gain additional side lobe suppression, which was not consciously applied, missing active antennas at the rim of the antenna array, or improper phase distribution. Besides the beam width, another remarkable point in the radiation pattern are the position and attenuation of nulls. The first null next to the main lobe, at about $4.3°$, is clearly seen in the simulations, but not as pronounced in the observations for the initially presented period of nominal functionality. A potential cause of this inferior behavior is assumed to be connected to random phase and amplitude variations over the antenna array. However, the position of the first null for the southwest-northeast cross-section is well accentuated for the shown period when container F failed and thus 20% of the transceiver modules were inoperable. Additionally, over the year we've seen transceiver modules and with this antennas randomly distributed over the antenna array got nonfunctional for the transmission case. At times up to 5% of the 433 transmitter modules are found defective temporarily or permanently that also impair the ideal radiation pattern, but are typically repaired during the next maintenance. In *Renkwitz* (2014) the influence of malfunctioning transceiver modules and thus the temporary loss of antenna array elements was examined as well as random amplitude and phase errors of all array elements. For the loss of 21 randomly distributed antenna modules a beam broadening of up to $0.2°$ was seen, while the position of the side lobes were mostly unchanged and just their absolute amplitudes varied. For random amplitude and phase errors ($\pm 1\,dB$ and $\pm 10°$) a negligible beam broadening was seen, but the intensity and positions of side lobes were significantly modified. Therefore, the estimated minor discrepancies seem to be well in line with the previously mentioned study.

More of concern seems to be the persistent and considerable underestimation of the side lobe intensity. With the unambiguous interferometric angular range of maximum $15.6°$ around the nominal beam position in this experiment, the main lobe and first three side lobes of transmit radiation pattern should be covered. In general, the observed lower count rates outside the main lobe correspond to the anticipated suppression of side lobes, though the derived intensity appears to be at least 5 dB too low. With the reasonably well shaped form of the main and side lobe derived from the occurrence rates, the meteor positions seem to be recovered reliably, which is connected to correct decoding and unwrapping the observed phases between the individual small subarrays used in the interferometric analysis. A systematically flawed determination of the meteor trajectories would directly result in an anomalous shape of the contour maps.

The most likely cause for the seen overestimated side lobe attenuation is probably related to the initial detection of meteor events, that is performed on the data of the entire antenna array. Meteor events off the nominal beam direction are already less frequently seen with the entire antenna array than it is with a smaller subarray like Anemones. The reasoning for the initial detection of meteor events using the entire array is related to the high likelihood to also detect the same event in all subarrays. Complementing the initial meteor detection by searching also in the Anemone and Hexagon data might provide a higher number of meteor events off the nominal beam position. The use of the simulated radiation pattern superposed of the entire array and an Anemone is still appropriate as can be seen by the beam width and the positions of side lobe and null. The superposition of the two-way radiation pattern of the entire array would result in a contradictory beam width of $2.4°$ rather than $3.6°$, and no indication for such severe broadening has been observed. Secondly, the contour of the main lobe rim at about -13 dB (greenish portion, see e.g. Figure 6) seem to form a hexagon, which is one radiation pattern characteristics of the Anemone subarrays.

The beam pointing accuracy was consistently estimated to be in the order of $0.12°$ southwestwards off the nominal beam direction for all examined data. A potential cause might be a slightly flawed phase calibration of the individual subarrays. Though, the effect of this error seems to be negligible as the nominal half-power beam width is almost forty times larger.

Noteworthy, other radar experiments facilitating an equivalent quality to verify the radiation pattern depend on either distinct scattering structures of known properties, which are rare for the wavelength used here, or highly sensitive receive-only observations of cosmic radio emissions and the ability to perform angular scans. With this, the generation of meteor head echo occurrence maps as a byproduct within standard monitoring experiments seems to be very adjuvant and provides valuable information about the health status of the radar and for validating the radiation pattern.

4 Conclusions

In this manuscript we presented analysis results for two periods of meteor head echo observations. The continuous operation of MAARSY with a multi-functional monitoring experiment also allows the extensive observation of meteor head echoes. The observation of meteor head echoes with MAARSY is motivated by performing the first continuous meteor head echo measurements to e.g. derive the climatology, radiant maps and investigate meteor showers in detail. As a byproduct of this rich dataset, the deduction of the radiation pattern was envisaged.

Earlier methods related the detected intensities of individual meteor head echo trajectories in piecewise comparisons to cross-sections of the simulated radiation pattern. Contrary, the method described here relies only on the derived positions of the meteor head echo trajectories, but not on the detected intensities. The angular distribution of meteor head trajectories and count rates for $0.2\text{x}0.2°$ bins are determined and occurrence maps are generated. These occurrence maps are assumed to be highly equivalent to the combined two-way radiation pattern.

For the cases shown in this study, a zenith beam and a 12.4° tilted beam were used during normal operation of the entire array and a period when about 20% of the transceiver modules failed, which mainly influenced the transmission pattern. The occurrences during these periods and the individual beams were compared to the simulated radiation pattern, which revealed a remarkable good agreement. Especially, for the one week lasting period of restricted functionality, the derived occurrence map matches exceptionally well to the simulations with its deformation of the main lobe and emerging side lobes. A minor deficiency seems to be existent in the derived absolute intensity of the side lobes which is most likely related to the involved meteor detection method basing on the measurements with the entire antenna array.

Nevertheless, the obvious performance of this method makes it to a very sensitive and reliable tool to monitor the radar system's health as a byproduct, which was underlined by the occurrence map derived for just one single day.

Acknowledgements. The authors explicitly acknowledge the contribution of Jorge L. Chau for adjuvant discussions and suggestions related to the interferometric analysis in general and to meteor head echo observations as well as Svenja Sommer who was involved in deriving absolute calibration phases for MAARSY. Furthermore, we express our gratitude to the Andøya Space Center for their permanent support for the operation and maintenance of the MAARSY radar. The radar development was supported by the german grant 01 LP 0802A of Bundesministerium für Bildung und Forschung, while the meteor head echo observations are supported by the grant STO 1053/1-1 of the Deutsche Forschungsgemeinschaft (DFG).

References

Chau, J. L., and R. F. Woodman (2004), Observations of meteor-head echoes using the Jicamarca 50 MHz radar in interferometer mode, *Atmospheric Chemistry and Physics*, *4*(2), 511–521, doi:10.5194/acp-4-511-2004.

Chau, J. L., F. R. Galindo, C. J. Heinselman, and M. J. Nicolls (2009), Meteor-head echo observations using an antenna compression approach with the 450 MHz Poker Flat Incoherent Scatter Radar, *Journal of Atmospheric and Solar-Terrestrial Physics*, *71*, 636–643, doi:10.1016/j.jastp.2008.08.007.

Chau, J. L., T. Renkwitz, G. Stober, and R. Latteck (2014), MAARSY multiple receiver phase calibration using radio sources, *Journal of Atmospheric and Solar-Terrestrial Physics*, *118*, 55–63, doi:10.1016/j.jastp.2013.04.004.

de Oliveira-Costa, A., M. Tegmark, B. M. Gaensler, J. Jonas, T. L. Landecker, and P. Reich (2008), A model of diffuse galactic radio emission from 10 MHz to 100 GHz, *Monthly Notices of the Royal Astronomical Society*, *338*, 247–260, doi:10.1111/j.1365-2966.2008.13376.x.

Fritts, D. C., D. Janches, H. Iimura, W. K. Hocking, N. J. Mitchell, R. G. Stockwell, B. Fuller, B. Vandepeer, J. Hormaechea, C. Brunini, and L. H. (2010), Southern argentina agile meteor radar: System design and initial measurements of large-scale winds and tides, *Journal of Geophysical Research: Atmospheres*, *115*, doi:10.1029/2010JD013850.

Fritts, D. C., D. Janches, H. Iimura, W. K. Hocking, J. V. Bageston, and N. M. Pene (2012), Drake antarctic agile meteor radar (draamer) first results: Configuration and comparison of mean and tidal wind and gravity wave momentum flux measurements with saamer, *Journal of Geophysical Research: Atmospheres*, *117*, doi:10.1029/2011JD016651.

Janches, D., J. D. Mathews, D. D. Meisel, and Q. H. Zhou (2000), Micrometeor observations using the Arecibo 430MHz radar I. Determination of ballistic parameter from measured Doppler velocity and deceleration results, *Icarus*, *145 (2)*, 53–63, doi:10.1006/icar.1999.6330.

Kero, J., C. Szasz, T. Nakamura, D. D. Meisel, M. Ueda, Y. Fujiwara, T. Terasawa, H. Miyamoto, and K. Nishimura (2011), First results from the 2009-2010 mu radar head echo observation programme for sporadic and shower meteors: the orionids 2009, *Monthly Notices of the Royal Astronomical Society*, *416*, 2550–2559, doi:10.1111/j.1365-2966.2011.19146.x.

Kero, J., C. Szasz, T. Nakamura, T. Terasawa, H. Miyamoto, and K. Nishimura (2012), A meteor head echo analysis algorithm for the lower VHF band, *Annales Geophysicae*, *30*(4), 639–659, doi:10.5194/angeo-30-639-2012.

Latteck, R., and I. Strelnikova (2015), Extended observations of polar mesosphere winter echoes over andøya (69°n) using MAARSY, *Journal of Geophysical Research: Atmospheres*, *120*(16), 8216–8226, doi:10.1002/2015JD023291, 2015JD023291.

Latteck, R., W. Singer, M. Rapp, B. Vandepeer, T. Renkwitz, M. Zecha, and G. Stober (2012), The new MST radar on Andøya: System description and first results, *Radio Science*, *47*, doi:10.1029/2011RS004775.

Nakamura, T., T. Tsuda, M. Tsutsumi, K. Kita, T. Uehara, S. Kato, and S. Fukao (1991), Meteor wind observations with the mu radar, *Radio Science*, *26*, 857–869, doi:10.1029/91RS01164.

Pellinen-Wannberg, A. (2005), Meteor head echoes - observations and models, *Annales Geophysicae*, *23*(1), 201–205, doi:10.5194/angeo-23-201-2005.

Pellinen-Wannberg, A., and G. Wannberg (1994), Meteor observations with the European Incoherent Scatter UHF Radar, *J. Geophys. Res.*, *99(A6)*, 11,379–11,390, doi:10.1029/94JA00274.

Renkwitz, T. (2014), Evaluation and validation of a novel MST-Radar for studying atmospheric 3D structures, Ph.D. thesis, University of Rostock.

Renkwitz, T., W. Singer, R. Latteck, G. Stober, and M. Rapp (2012), Validation of the radiation pattern of the Middle Atmosphere Alomar Radar System (MAARSY), *Advances in Radio Science*, *10*, 245–253, doi:10.5194/ars-10-245-2012.

Atmos. Meas. Tech. Discuss., doi:10.5194/amt-2016-320, 2016
Manuscript under review for journal Atmos. Meas. Tech.
Published: 7 October 2016

Renkwitz, T., G. Stober, R. Latteck, W. Singer, and Rapp (2013), New experiments to validate the radiation pattern of the Middle Atmosphere Alomar Radar System (MAARSY), *Advances in Radio Science*, *11*, 283–289, doi:10.5194/ars-11-283-2013.

Renkwitz, T., C. Schult, R. Latteck, and G. Stober (2015), Validation of the radiation pattern of the VHF MST radar MAARSY by scattering off a sounding rocket's payload, *Advances in Radio Science*, *13*.

Schult, C., G. Stober, J. L. Chau, and R. Latteck (2013), Determination of meteor-head echo trajectories using the interferometric capabilities of MAARSY, *Ann. Geophys.*, *31*, 1843–1851, doi:10.5194/angeo-31-1843-2013.

Schult, C., G. Stober, J. L. Chau, and D. Janches (2016), Results of the first continuous meteor head echo survey at polar latitudes, *Icarus*, submitted.

Sommer, S., G. Stober, and J. L. Chau (2016), On the angular dependence and scattering model of polar mesospheric summer echoes at vhf, *Journal of Geophysical Research: Atmospheres*, *121*(1), 278–288, doi:10.1002/2015JD023518, 2015JD023518.